Title

Retinal imaging demonstrates reduced capillary density in clinically unimpaired APOE ε4 gene carriers

Journal

Alzheimer's & Dementia Diagnosis Assessment & Disease Monitoring, 13(1)

ISSN

2352-8729

Authors

Elahi, Fanny M
Ashimatey, Senyo B
Bennett, Daniel J
et al.

Publication Date

2021

DOI

10.1002/dad2.12181

Peer reviewed

Received: 23 September 2020 | Revised: 2 March 2021 | Accepted: 5 March 2021 | Published online: 8 April 2021

DOI: 10.1002/dad2.12181

Alzheimer's & Dementia
Diagnosis, Assessment & Disease Monitoring

RESEARCH ARTICLE

Retinal imaging demonstrates reduced capillary density in clinically unimpaired *APOE ε4* gene carriers

Fanny M. Elahi[1,2] | **Senyo B. Ashimatey**[3] | **Daniel J. Bennett**[4] | **Samantha M. Walters**[1] | **Renaud La Joie**[1] | **Xuejuan Jiang**[3] | **Amy Wolf**[1] | **Yann Cobigo**[1] | **Adam M. Staffaroni**[1] | **Howie J. Rosen**[1] | **Bruce L. Miller**[1] | **Gil D. Rabinovici**[1,5] | **Joel H. Kramer**[1] | **Ari J. Green**[4,6] | **Amir H. Kashani**[3,7]

[1] Department of Neurology, Memory and Aging Center, Weill Institute for Neurosciences, San Francisco, University of California, San Francisco, California, USA

[2] San Francisco Veterans Affairs Health Care System, San Francisco, California, USA

[3] Department of Ophthalmology, USC Roski Eye Institute, Keck School of Medicine of the University of Southern California, Los Angeles, California, USA

[4] Department of Neurology, Division of Neuroimmunology and Glial Biology, Weill Institute for Neurosciences, San Francisco, University of California, San Francisco, California, USA

[5] Department of Radiology and Biomedical Imaging, San Francisco, University of California, San Francisco, California, USA

[6] Department of Ophthalmology, San Francisco, University of California, San Francisco, California, USA

[7] USC Ginsberg Institute for Biomedical Therapeutics, Los Angeles, California, USA

Correspondence
Fanny M. Elahi, Memory and Aging Center, Weill Institute for Neurosciences, 675 Nelson Rising Lane, Suite 190, San Francisco, CA 94158, USA.
E-mail: fanny.elahi@ucsf.edu, elahi-lab15@gmail.com
Amir H. Kashani, Wilmer Eye Institute, Johns Hopkins School of Medicine, 600 N Wolfe St., Baltimore, MD 21287, USA.
E-mail: akashan1@jhmi.edu

Both F.M.E. and A.H.K. contributed equally to this work as senior authors.

Abstract

Introduction: Apolipoprotein E (*APOE*) ε4, the strongest non-Mendelian genetic risk factor for Alzheimer's disease (AD), has been shown to affect brain capillaries in mice, with potential implications for AD-related neurodegenerative disease. However, human brain capillaries cannot be directly visualized in vivo. We therefore used retinal imaging to test *APOE* ε4 effects on human central nervous system capillaries.

Methods: We collected retinal optical coherence tomography angiography, cognitive testing, and brain imaging in research participants and built statistical models to test genotype–phenotype associations.

Results: Our analyses demonstrate lower retinal capillary densities in early disease, in cognitively normal *APOE* ε4 gene carriers. Furthermore, through regression modeling with a measure of brain perfusion (arterial spin labeling), we provide support for the relevance of these findings to cerebral vasculature.

Discussion: These results suggest that *APOE* ε4 affects capillary health in humans and that retinal capillary measures could serve as surrogates for brain capillaries, providing an opportunity to study microangiopathic contributions to neurodegenerative disorders directly in humans.

KEYWORDS
Alzheimer's disease, apolipoprotein E ε4, capillary rarefaction, preclinical biomarker, preclinical disease, vascular contributions to Alzheimer's disease

1 | INTRODUCTION

It has become increasingly clear that Alzheimer's disease (AD) is not strictly a disorder of neuronal dysfunction but that changes in vasculature could play an important role in disease pathogenesis.[1–6] The most prevalent genetic risk for AD remains the ε4 allelic variant of apolipoprotein E (*APOE*), a gene systemically involved in lipid metabolism and vascular health, including cerebral vasculature.[7–10]

In autopsy studies, vascular changes are among the most common co-pathologies in subjects harboring *APOE* ε4 and AD neuropathological changes.[11–13] Genetic studies, including pleiotropy analyses, suggest shared genetic risk among vascular disease, lipid metabolism, and AD.[4] *APOE* ε4 is a prominent genetic example of this shared vulnerability.[5] The exact mechanisms by which *APOE* ε4 contributes to AD pathogenesis remains an active area of research. Studies in model systems[14,15] and human epidemiological investigations[16] suggest that *APOE* ε4-mediated neurodegeneration is related to vascular pathology.[5] It remains unclear, however, which vessels are most prominently affected by *APOE* ε4 in humans and how the pathological changes contribute to AD neuropathology. The largest community-based neuropathological study of *APOE* ε4 reported a higher prevalence of large-vessel atherosclerosis in *APOE* ε4 gene carriers.[17] However, due to technical limitations, most historical human autopsy studies have been limited to investigating larger caliber vessels. Recent studies in mouse models harboring human *APOE* ε4 alleles demonstrate capillary pathology, along with blood-brain barrier (BBB) leakage and dysfunction of the neurovascular unit (NVU).[14,15,18,19]

APOE ε4 may be affecting capillaries via endothelial or pericytic changes, but a more likely possibility is multicellular dysfunction of the BBB and NVU, and dysregulated clearance of toxic metabolic byproducts of brain function. On average, *APOE* ε4 carriers, especially female carriers, have a higher cerebral amyloid burden. Sex-dependent differences in amyloidopathy and other neuropathological components of AD are an active area of research. *APOE* ε4-associated amyloidopathy, in specific, may in part be related to deficiencies in cerebral clearance mechanisms.[20] Recently, oligomeric amyloid has been shown to cause capillary disease (constriction) via an effect on vascular pericytes,[21] master regulators of capillary function. Importantly, more than a decade prior to these studies, Salloway et al. reported a dose-dependent *APOE* ε4 effect on the microvascular basement membrane of the frontal cortex in 35 AD brains.[22] These pathological changes could be reactive or causative. However, the combination of these studies with mechanistic interventions in model systems,[14,15] and human epidemiological studies,[16] provides strong support for vascular contributions to *APOE* ε4-associated neurodegenerative disease, and likely one that affects microvasculature.

Despite strong evidence that *APOE* ε4 is associated with microangiopathy,[14,15] and that this pathology may be an important contributor to AD pathogenesis[23–25] (reviewed in Sweeney et al.[26]), it is currently not technically feasible to individually visualize brain microvessels in living humans. The retina is an extension of central nervous system (CNS) tissue, constituted by neurons and glia, and the retinal microvasculature can be visualized in vivo at a high resolution with optical coherence tomography angiography (OCTA).[27,28] OCTA is a noninvasive, rapid, and US Food and Drug Administration (FDA) approved imaging modality that can provide high resolution images of retinal capillaries by detecting the variable scatter of light from moving red blood cells compared to non-moving neuroretinal tissue.[29–31] Abnormal retinal capillary function has been reported in subjects with early or subclinical retinal vascular diseases, including diabetes[32] and hypertension.[33] In patients with advanced AD, OCTA has demonstrated significantly lower retinal capillary density.[34] In the current study, we leveraged the established sensitivity of OCTA for subclinical capillary pathology to investigate *APOE* ε4-associated capillary disease in asymptomatic gene carriers at risk for AD. Subsequently, we investigated the specific association of retinal capillary measures with arterial spin labeling (ASL) magnetic resonance imaging (MRI), a measurement of cerebral blood flow (CBF), as a means of testing the relevance of retinal vessel measures to global brain perfusion.

RESEARCH IN CONTEXT

1. Systematic review: The authors reviewed the available scientific literature on PubMed for articles examining retinal biomarkers in cognitively normal apolipoprotein E (*APOE*) ε4. While abundant studies examine retinal "biomarkers" for clinically impaired individuals with Alzheimer's disease (AD), we did not find any studies investigating *APOE* ε4-associated retinal vascular changes in preclinical disease stage. In this study, we investigated the microangiopathy associated with *APOE* ε4 carrier status and demonstrate the relevance of retinal findings by showing associations with brain perfusion. The association of *APOE* ε4 with capillary rarefaction was not dependent on amyloid burden.
2. Interpretation: We show that *APOE* ε4 is associated with age-dependent capillary rarefaction. Given the importance of *APOE* ε4 for AD, this work strongly suggests that small vessel disease may occur early, in the preclinical stage of disease, and play an important role in the risk of AD at least in *APOE* ε4 carriers.
3. Future directions: Longitudinal studies of retinal and brain imaging in *APOE* ε4 cohorts, including individuals who convert from cognitively normal to cognitively impaired, will help decipher causality of vascular abnormalities. Studies in model systems will also help elucidate mechanisms.

2 | METHODS

2.1 | Study participants and design

Consecutive enrollment of research participants from January 11, 2018 to April 8, 2019 was undertaken from ongoing longitudinal

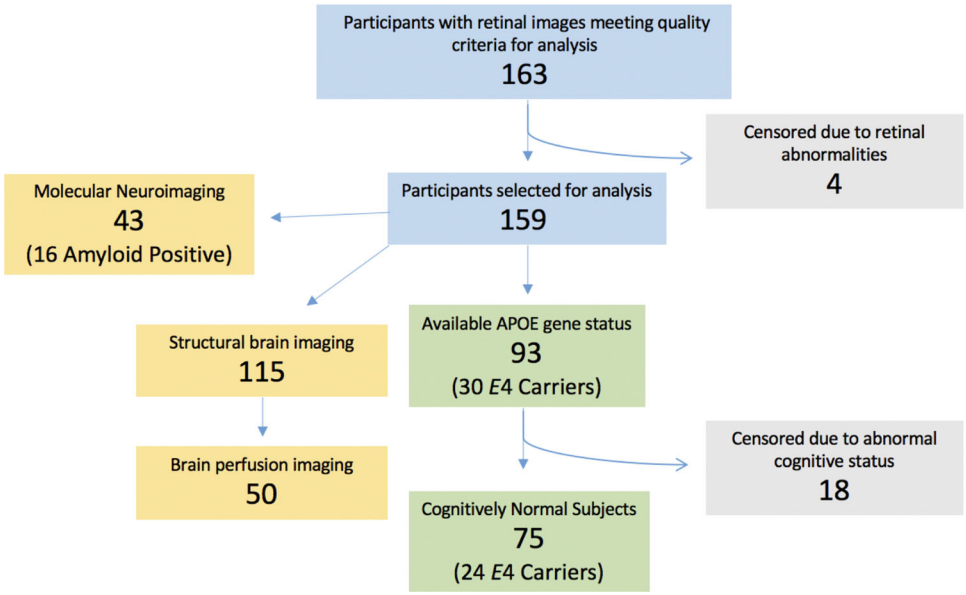

FIGURE 1 Study design. Study design flowchart, including subject recruitment (blue box) and censorship (gray box). Green boxes represent data used for primary analyses of apolipoprotein E ε4 genetic associations with retinal capillary morphometric measures; yellow boxes represent available data used in secondary analyses such as structural brain imaging, perfusion imaging, and molecular neuroimaging

studies of brain aging and neurodegenerative disease at the Memory and Aging Center at University of California San Francisco (UCSF; National Institute of Health [NIH]-funded studies: Aging and Cognition, Chronic Inflammation, MarkVCID studies, and Alzheimer's Disease Research Center; and Larry L. Hillblom Foundation Aging Network study) into our prospective study (N = 272) in the UCSF Visual Neurodiagnostics Laboratory. All study participants had a measure of functional impairment (informant Clinical Dementia Rating [CDR]), extensive neuropsychological testing, physical examination, and demographic information, while the majority had vascular disease risk factor measures (blood pressure; body mass index [BMI]; history of hyperlipidemia, hypertension, and diabetes) and brain imaging (Figure 1). Exclusion criteria of parent studies also applied to this study, including active or uncontrolled psychiatric disease such as psychosis, brain tumor, or history of brain surgery; in addition, we required absence of any clinically significant ophthalmological abnormalities, such as glaucoma, visually significant cataract, macular degeneration, or cystoid macular edema. Given our interest in associations of *APOE* ε4 with microvascular changes prior to neurodegenerative symptom presentation, our primary analyses were limited to the subgroup of cognitively normal participants (n = 75) defined as those individuals who had cognitive test scores within normal range for age and level of educational attainment and no study partner concern (CDR = 0). All study participants provided informed consent and the study protocols were approved by the UCSF Human Research Protection Program and Institutional Review Board. Research was performed in accordance with the Code of Ethics of the World Health Organization. Compared to participants without genomic DNA (n = 66), participants with genomic DNA for *APOE* genotype (N = 93) were more likely to be 75 years and older (P = .01), but similar in sex, race, years of education, and history of hypertension and diabetes (P > .05 for all).

2.2 | Optical coherence tomography angiography and retinal capillary density quantification

OCTA images were acquired with a commercially available and FDA-approved Spectral Domain (SD) OCTA system—Cirrus HD-OCT (Carl Zeiss Meditec, Inc.). This system uses a light source with wavelength 840 nm and acquires 68,000 A-scans per second. The highest resolution 3 × 3 mm^2 scan, which has 245 B-scans in the horizontal plane, were used for all analyses. The axial and transverse resolution of the scan pattern are 5 and 15 μm, respectively. Each B-scan was consecutively repeated at least three times at acquisition and the scan with the best image quality from either eye of a subject was selected for analysis. OCTA scans were performed at UCSF and reviewed for quality by an experienced OCTA technician at USC who was masked to *APOE* genotype and to all clinical measures, and had no knowledge of the results of brain imaging and neurocognitive assessments performed at UCSF. Only retinal scans with signal strength greater than 7 and otherwise good quality, including centeredness of the scan on the fovea and minimal to no motion artifacts, were used for analyses (n = 159; Figure 1). A previously validated semiautomated software program written in MATLAB (R2018b; MathWorks, Inc.) was used to analyze OCTA images.[35–38] To avoid the potential confounding effect of projection artifacts, only the superficial retinal layer of the image was segmented and used for our primary analysis. The superficial retinal layer includes the retinal nerve fiber layer, ganglion cell layer, and inner plexiform layer. We and others have previously described several measures of retinal capillary density and morphology.[35,36] In this study, we report the most simple and direct measures of retinal capillary density, termed vessel area density (VAD) and vessel skeleton density (VSD). VAD is derived from a binarized raw OCTA image of the superficial retinal layer and represents the total area of the image that

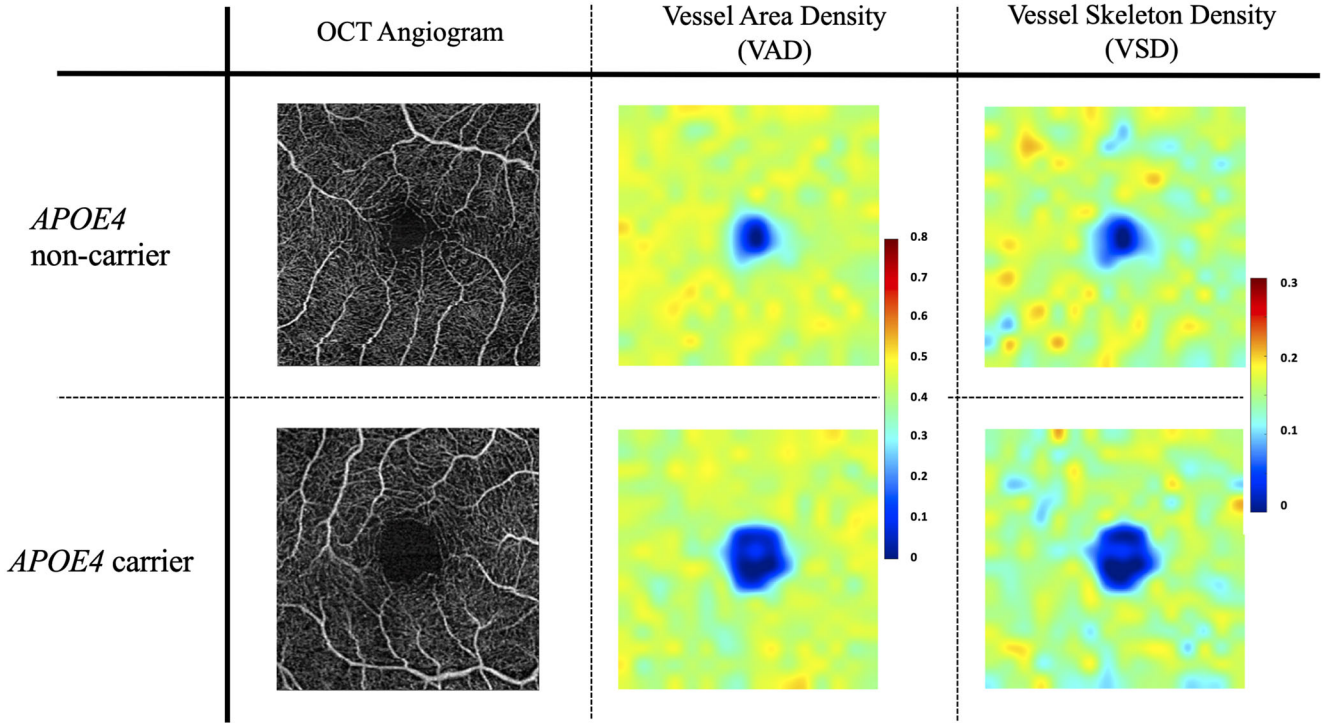

FIGURE 2 Single subject comparison of optical coherence tomography angiography (OCTA) scans in a carrier versus noncarrier. Retinal capillary density maps derived from OCTA images for an apolipoprotein E (*APOE*) ε4 carrier and non-carrier. The first column shows raw OCTA images where white pixels represent retinal vessels within a 3 × 3 mm^2 region surrounding the naturally occurring foveal avascular zone of the retina. The second and third columns represent pseudo-colored capillary density heat maps of the same images using either the vessel skeleton density or vessel area density metrics. Hot colors depict regions of higher capillary density. Rows represent a single subject comparison of capillary density between a heterozygote for *APOE* ε4 (bottom row) versus a noncarrier (top row), matched by demographic and vascular risk factors. Both are females, aged 72 years, with body mass index of 21 kg/m^2. The APOE ε4 noncarrier had numerous focal regions of greater retinal capillary density (red) throughout the retina as well as a smaller foveal avascular zone compared to the APOE ε4 carrier

is occupied by blood flow signal.[36] VSD is computed from a binarized OCTA image in which the vessels are reduced to a single pixel thickness and then divided by the total area of the image. VSD provides a measure of the length of vessels present within an image.[36] Both methods of assessing capillary density are complementary. Examples of OCTA image and capillary density metrics are shown in Figure 2. Additional details on the OCTA metrics can be found elsewhere.[27,32,35,36,38]

2.3 | Brain imaging acquisition and processing

MRI scans were acquired on a 3T MRI scanner Prisma Fit (Siemens AG). Volumetric MPRAGE sequences at UCSF were used to acquire T1-weighted images of the entire brain (sagittal slice orientation; slice thickness = 1.0 mm; slices per slab = 160; in-plane resolution = 1.0 × 1.0 mm; matrix = 240 × 256; TR = 2,300 ms; TE = 2.9 ms; TI = 900 ms; flip angle = 9°).[39] Pseudo-continuous ASL (pcASL) images were acquired using the recommendations described by Alsop et al.[40] pcASL-MRI was performed with TR/TE = 4050/34 ms, labeling duration of 1500 ms, and postlabeling delay of 1800 ms. Each slice is 3 mm thick with a 2.5 × 2.5 mm^2 in-plane resolution. Quality control included visual inspection of all images. Images with excessive motion or image artifact were excluded. T1-weighted images underwent bias field correction using an N3 algorithm, and the segmentation was performed using SPM12 (Wellcome Trust Center for Neuroimaging, London, UK, http://www.fil.ion.ucl.ac.uk/spm) unified segmentation.[41] A group template was generated from the segmented gray and white matter tissues and cerebrospinal fluid by non-linear registration template generation using large deformation diffeomorphic metric mapping framework.[42] Native subjects space gray and white matter were normalized, modulated, and smoothed in the group template. The applied smoothing used a Gaussian kernel with 8 mm full width half maximum. Every step of the transformation was carefully inspected from the native space to the group template. For statistical purposes, linear and non-linear transformations between the group template space and International Consortium for Brain Mapping (ICBM) was applied.[43] Quantification of volumes in specific brain regions at each time point was accomplished by transforming a standard parcellation atlas[44] into ICBM space and summing all modulated gray matter within each parcellated region. Total intracranial volume (TIV) was estimated for each subject in Montreal Neurological Institute (MNI) space.[45] Gray matter volume (GMV) and TIV are reported in cm^3. ASL was processed to obtain partial volume corrected maps of gray matter perfusion as previously described.[46–48] Frames of the ASL acquisition were corrected for motion, coregistered with the first frame (M0) using FSL (FMRIB Software Library),[49] and differential perfusion images were created by

subtracting unlabeled frames from adjacent labeled frames and averaging these subtraction images.[50] Susceptibility artifacts along the phase-encoding direction were corrected in the M0 frame and perfusion map using Advanced Normalization Tools image registration (ANTs SyN)[51] restricted to the coronal axis. An automatic quality control process removed tagged/untagged pairs of frames when the relative root mean square (RMS) distance value between two consecutive frames was higher than 0.5 mm. The participant was dropped if this RMS value was higher than 1 mm. CBF was calculated by applying the Buxton kinetic model to the perfusion map.[52,53] Partial volume correction was based on the tissue segmentation maps from MPRAGE using the transformation matrix from T1 to M0.[46,54] All CBF images were visually inspected in the native and MNI spaces. Poor quality images that were out of the field of view or contained large susceptibility or motion artifacts were removed from the study.

2.4 | Molecular neuroimaging (amyloid positron emission tomography)

Amyloid-positron emission tomography (PET) results on 43 subjects were used to assess amyloid-associated differences in retinal microvasculature. PET was acquired with either ^{11}C-Pittsburgh compound B (PiB, acquired on a Siemens Biograph PET/CT scanner, $n = 9$, or a ECAT EXACT HR PET scanner, $n = 1$) or ^{18}F-florbetapir (on a GE Discovery STE/VCT PET-CT, $n = 33$). PiB pre-processing and acquisition followed previously described methods.[51] Briefly, we used PiB-PET data acquired between 50 and 70 minutes post injection as four 5-minute frames; frames were realigned, averaged, coregistered to the closest available MRI, and scaled using the cerebellar cortex as a reference region (based on FreeSurfer segmentation) to obtain standardized uptake value ratio (SUVR) images. Florbetapir was acquired between 50 and 70 minutes post injection as four 5-minute frames and processed following Alzheimer's Disease Neuroimaging Initiative procedures (http://adni.loni.usc.edu/methods/pet-analysis-method/pet-analysis/). Frames were smoothed to a final 8 mm isotropic resolution, realigned, averaged, coregistered to the closest available MRI, and scaled using the whole cerebellum (gray and white matter) as a reference region to obtain SUVR images. For both tracers, FreeSurfer segmentation of the cortical mantle was used to define a cortical composite region encompassing frontal, cingulate, parietal, and lateral temporal areas from which the average SUVR value was extracted as a measure of neocortical amyloid beta burden. To determine amyloid status, tracer- and preprocessing-SUVR thresholds derived from previous publications were applied (1.21 for PiB,[55] and 1.11 for florbetapir[56]). These thresholds have been validated compared to a *post mortem* gold standard.[55–58]

2.5 | Statistical analyses

The primary analysis investigated the influence of *APOE* ε4 genotype on retinal capillary density using analysis of covariance (ANCOVA) controlling for the effects of age, sex, and quantified vascular risk factors (systolic blood pressure [SBP] and BMI). To better understand the relationship between age and capillary density in our model, we investigated age as a predictor of capillary density in *APOE* ε4 carriers and non-carriers independently, using separate linear models without the addition of covariates. Finally, we used a multivariate hierarchical linear regression approach to understand the predictive value added by basic demographics (model 1); basic demographics and vascular risk factors (model 2); and basic demographics, vascular risk factors, and *APOE* gene status (model 3). Only the eye with highest OCTA quality from each participant was selected for analysis. Analyses were repeated in the other eye to ensure that a selection bias was not introduced. Statistical significance was defined at an alpha level of $P = .05$.

In secondary analyses, we aimed to demonstrate a correlation between OCTA measures of retinal vascular density, and MRI measures of global CBF, as a proof of concept that the two measurements are related. All subjects with retinal and brain imaging, regardless of phenotype and degree of impairment, were included in the analysis. Multivariate linear regression models were used to assess the relation between retinal capillary density and CBF, total gray matter volumes (GMV), white matter volumes (WMV), and mean hippocampal volumes (HIP, averaged between the left and right hippocampus), controlling for TIV, and in the case of CBF, also controlling for sex. Due to the similarities of aging effect, an important variable that influences the dynamics of retinal and CBF and neurodegeneration, age was not compensated in this analysis. For similar reasons, vascular risk factors were also not compensated.

To ensure that missing data did not alter results and our inferences, we re-ran statistical models using imputed values for Mini-Mental Status Examination (MMSE), heart rate, systolic and diastolic blood pressure, and BMI. We imputed missing values using the least squares prediction method.

3 | RESULTS

3.1 | Demographics

Participant characteristics are summarized in Table 1. No significant differences were found in age or vascular risk factors between *APOE* ε4 carriers and noncarriers ($P = .27$). In addition, there were no significant differences with respect to sex and educational attainment between groups. Measures of cognitive function, and functional independence (CDR) were similar as well (Table 1). Thirty-two percent (24/75) of the cognitively normal study cohort were *APOE* ε4 carriers (2 ε4/ε4, 2 ε2 ε4, and 20 ε3/ε4).

3.2 | APOE ε4 is associated with decreased capillary density in cognitively normal older adults

Controlling for comorbidities and vascular risk factors, group comparisons of *APOE* ε4 carriers versus noncarriers revealed significantly

TABLE 1 Summary of demographic and basic clinical data by APOE status in the primary analysis cohort

	APOE ε4 negative	APOE ε4 positive	*P*-value
n	51	24	n/a
Age - median [range]	75 [37–90]	72 [26–83]	.474
Female - *n* (%)	33 (65)	12 (50)	.337
Education years - mean (SD)	17.4 (2.2)	17.0 (2.1)	.432
missing - *n* (%)	3 (6)	3 (12)	
Body mass index - mean (SD)	25.5 (3.8)	23.8 (2.8)	.067
missing - *n* (%)	8 (16)	3 (12)	
Systolic blood pressure - mean (SD)	131.1 (15.4)	136.9 (15.6)	.164
missing - *n* (%)	9 (18)	3 (12)	
Diastolic blood pressure - mean (SD)	73.7 (9.1)	73.3 (6.9)	.858
missing - n (%)	9 (18)	3 (12)	
Heart rate - mean (SD)	69.4 (9.8)	69.5 (13.4)	.987
missing - *n* (%)	9 (18)	3 (12)	
Clinical Dementia Rating - mean (SD)	0.0 (0.0)	0.0 (0.0)	n/a
Mini-Mental State Examination score - mean [range]	29 [26–30]	30 [25–30]	.521
missing - *n* (%)	10 (20)	3 (12)	
Structural brain imaging analysis - included/not included (%)	43/8 (84/16)	17/7 (71/29)	.293
Cerebral blood flow analysis - included/not included (%)	18/33 (35/65)	12/12 (50/50)	.337
Molecular neuroimaging analysis - included/not included (%)	18/33 (35/65)	7/17 (29/71)	.793

Notes: Summary statistics of the demographic, medical information, and secondary analysis group inclusion for the subjects with known *APOE* ε4 gene status. Normally distributed variables are characterized by mean and standard deviation (mean [SD)]), while skewed variables are characterized by median and range (median [range]). *P*-values represent *t* test for normally distributed variables and Mann-Whitney *U* tests for skewed variables. Within the *APOE* ε4 positive group, two participants were homozygote for the *APOE* ε4 allele.
Abbreviations: APOE, apolipoprotein E; SD, standard deviation.

lower capillary density in carriers with large effect sizes for both measures of density: VAD ($F[1,62] = 16.99$, $P = .0001$; partial eta squared = 0.22; Figure 3.A.) and VSD ($F[1,62] = 11.52$, $P = .001$; partial eta squared = 0.16; Figure 3.B.). Reduced capillary density between *APOE* ε4 carriers and noncarriers could be directly visualized comparing participants matched by age, sex, and BMI (Figure 2). Importantly, we found an age-dependent effect on retinal capillary density in *APOE* ε4 carriers (Figure 4).

Next, hierarchical regression models were built to demonstrate the effect of *APOE* ε4 on retinal capillaries beyond other vascular risk factors (Figure 5). Model 1 included demographic factors of age and sex as predictors of capillary density. In model 2, vascular risk factors were added to the demographic factors included in model 1, and in model 3, *APOE* ε4 status was added to the variables in model 2. Results support the importance of the *APOE* ε4 effect on vasculature, with a trivial increase in model fit with the addition of vascular risk factor to age (comparison of models 1 and 2) and a substantive increase with the inclusion of *APOE* ε4 in model 3. Specifically, for VAD, R^2 of .10 in model 2 increased to .29 in model 3, and for VSD, R^2 of 0.10 in model 2 increased to 0.24 in model 3. To determine the unique

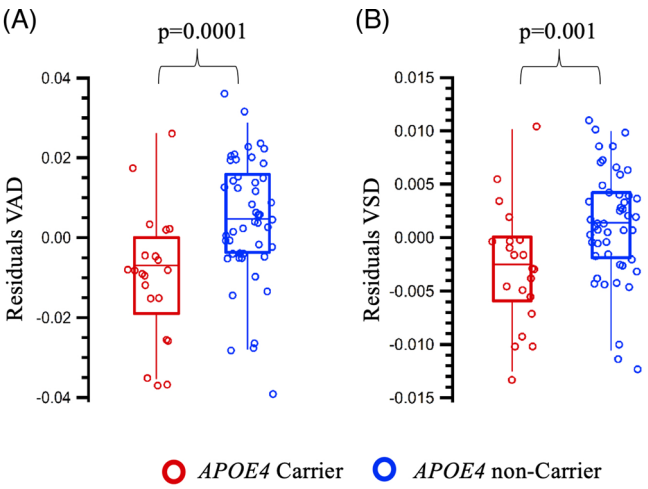

FIGURE 3 Retinal capillary density by apolipoprotein E (*APOE*) ε4 status. A comparison of *APOE* ε4 carriers (red) and non-carriers (blue) on residual measures of retinal capillary density (vessel area density [A] and vessel skeletal density [B]) after controlling for age, sex, systolic blood pressure, and body mass index

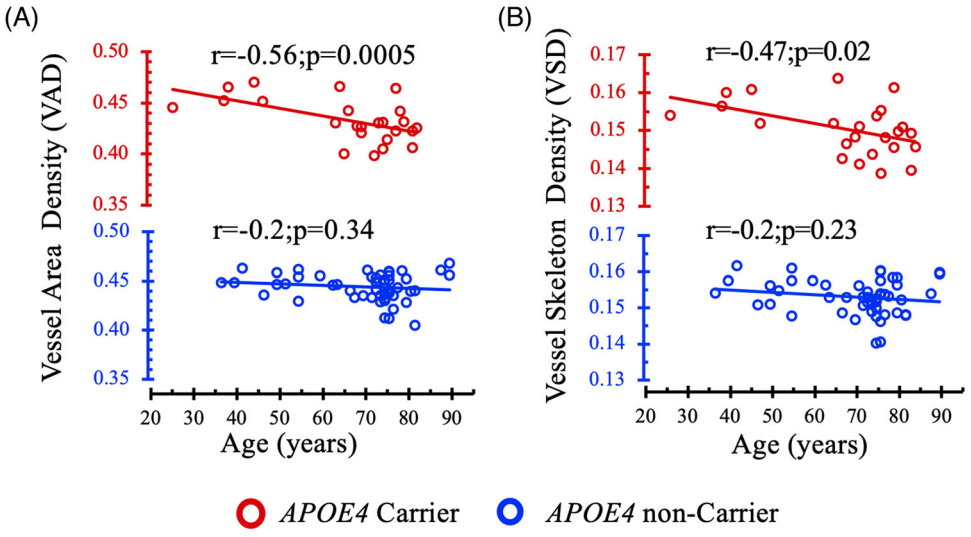

FIGURE 4 Association of age with retinal capillary densities. Association of two measures of retinal capillary density (vessel area density [A] and vessel skeleton density [B]) in apolipoprotein E (*APOE*) ε4 carriers (red) and noncarriers (blue)

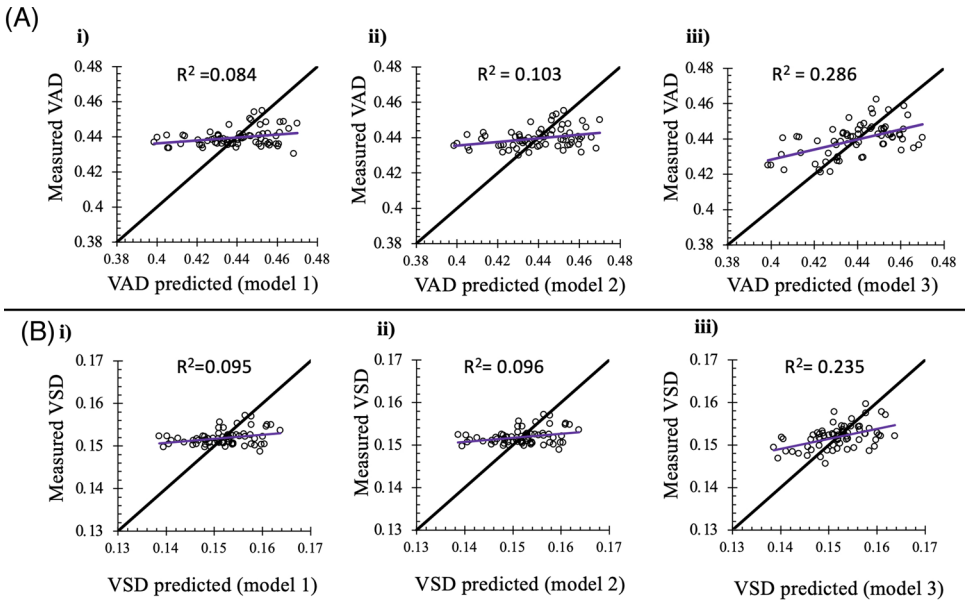

FIGURE 5 Hierarchical regression models to assess effect of apolipoprotein E (*APOE*) ε4 on retinal capillary densities. Step-wise assessment of the added value of *APOE* ε4 status in predicting two measures of retinal capillary density (vessel area density [A] and vessel skeleton density [B]) in cognitively normal individuals. A hierarchical regression model was built using (i) age and sex; (ii) age, sex, and quantifiable vascular risk factors (body mass index and systolic blood pressure); and (iii) age, sex, vascular risk factors, and *APOE* ε4 carrier status. *APOE* ε4 versus non-*APOE* ε4 genotype uniquely explained ≈18% of the variance in vessel area density and ≈14% of the variance in Vessel Skeletal Density. VAD , vessel area density; VSD , vessel skeleton density; R^2 = model fit

contribution of *APOE* ε4 *to* capillary density, the coefficient of determination of model 2 was deducted from that of model 3 to demonstrate that an *APOE* ε4 allele uniquely explains up 18% (P = .0001) and 14% (P = .001) of the variability in the VAD and VSD, respectively (Figure 5).

As noted earlier, primary analyses were limited to cognitively unimpaired individuals and only retinal scans passing stringent quality-based inclusion criteria were included in the analyses. Therefore, to rule out bias by censorship, analyses were cross-validated by including data from all subjects irrespective of the CDR score, and re-running analyses using the unselected eye in the primary cohort, including eyes that were not originally used for analysis due to quality-based exclusion. Similar findings were noted when participants with functional impairment (CDR score > 0) were included (Figure S1 in supporting

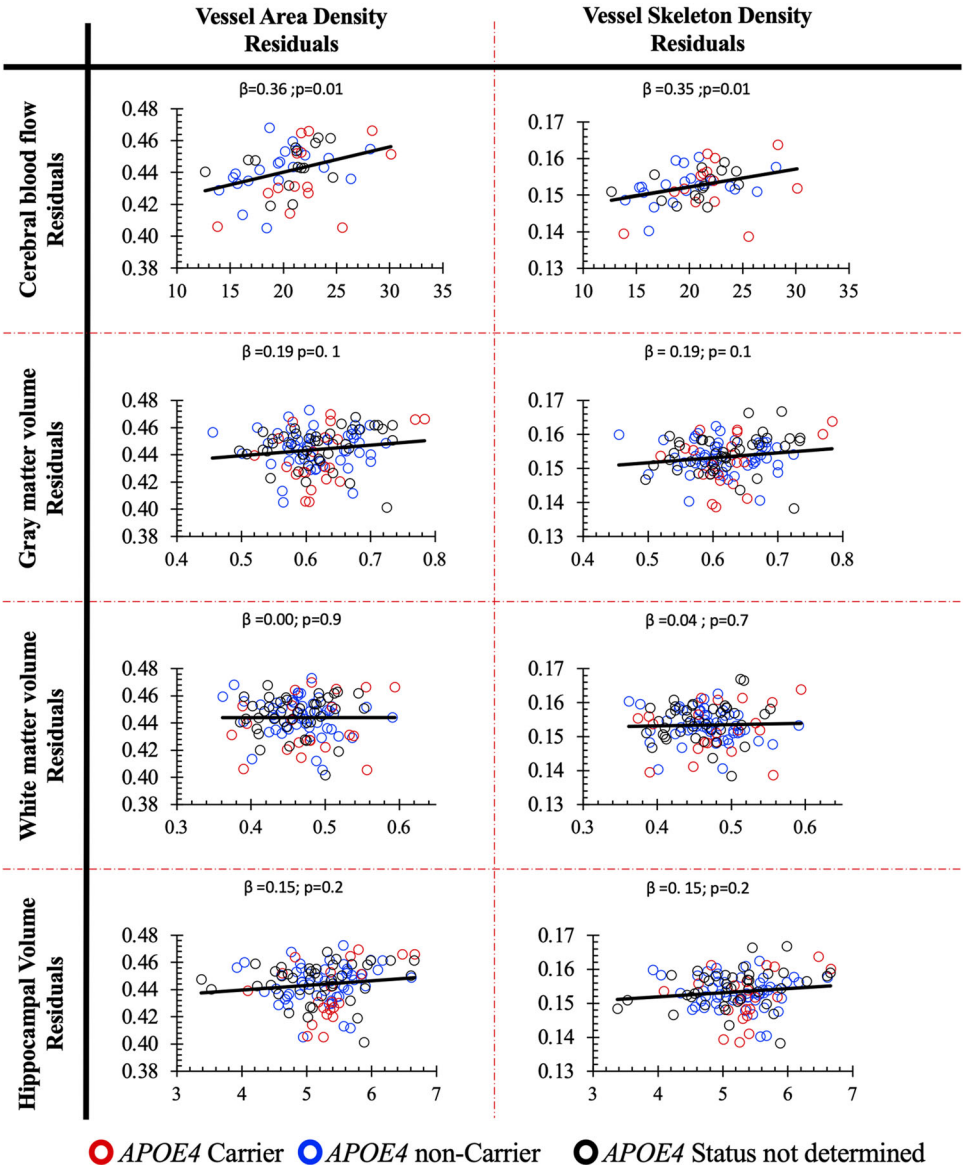

FIGURE 6 Association of retinal capillary densities with brain imaging measures. Association of two measures of retinal capillary density (vessel area density and vessel skeleton density) with cerebral blood flow, total gray matter volume, white matter volume, and hippocampal volume. All volumetric brain imaging measures were adjusted for total intracranial volume and cerebral blood flow was adjusted for both total intracranial volume and sex. Only cerebral blood flow was significantly associated with measures of retinal capillary density. These analyses include all subjects, regardless of cognitive status and apolipoprotein E (*APOE*) ε4 status (blue = noncarrier, red = *APOE* ε4 carrier, and black = unknown gene status)

information), as well as in analyses using the alternate eye (Figure S2 in supporting information).

Of note, to ensure that our inferences were not impacted by missing data, we confirmed all models in a complete, imputed dataset.

3.3 | Associations of retinal capillary density with neuroimaging measures

We found an association between retinal capillary density and CBF (VAD [$\beta = 0.36$, $P = .01$], VSD [$\beta = 0.35$, $P = .01$]; Figure 6). The correlation of retinal capillary density with gray matter volume (VAD [$\beta = 0.12$, $P = .1$]; VSD [$\beta = 0.12$, $P = .1$]), white matter volume (VAD [$\beta = 0.00$, $P = .9$]; VSD [$\beta = 0.03$, $P = .7$]) and hippocampal volume (VAD [$\beta = 0.12$, $P = .2$]; VSD [$\beta = 0.12$, $P = .2$]) were smaller in magnitude and not significant (Figure 6). Controlling for the effects of vascular risk factors in addition to sex yielded similar correlation magnitudes for the CBF analysis, with reduced *P*-values VAD ($r = 0.35$, $P = .03$) and VSD ($r = 0.32$,$P = .05$). As expected, however, when age was included as a covariate, the magnitude of the retinal vessel density correlation with CBF was small and non-significant (VAD [$r = 0.2$, $P = .16$] and VSD [$r = 0.15$,$P = .14$]). For retina-brain imaging associations we included our entire cohort, regardless of cognitive status (Table S1 in supporting information).

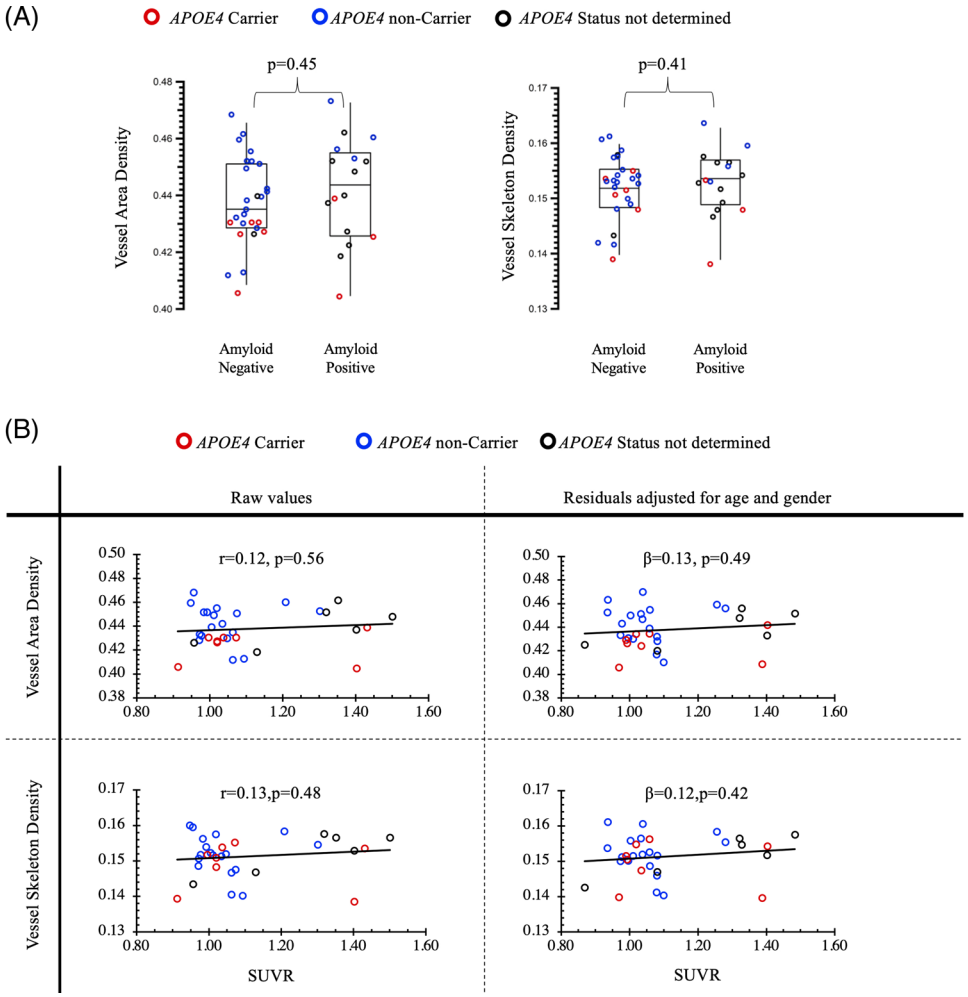

FIGURE 7 A, Retinal capillary density by cerebral amyloid group. A comparison of two measures of retinal capillary density (vessel area density and vessel skeleton density) between amyloid positive and amyloid negative subgroups controlling for age and sex. Amyloid status was determined by either 18F-florbetapir or 11C-Pittsburgh compound B standardized uptake value ratios. Analysis included all participants with available amyloid status, regardless of cognitive status and apolipoprotein E (*APOE*) ε4 status (blue = non-carrier, red = APOE ε4-carrier, black = unknown gene status). No significant relationships were found between amyloid status and retinal capillary density. B, Retinal capillary density regressions with cerebral amyloid positron emission tomography signal. Association of two measures of retinal capillary density (vessel area density and vessel skeleton density) with 18F-florbetapir standardized uptake value ratios (SUVR). Plots on the left present raw values, while plots on the right present residuals after controlling for age and sex. Analyses included all patients with available tracer uptake ratios, regardless of cognitive status or *APOE* ε4 status (blue = non0carrier, red = APOE ε4-carrier, black = unknown gene status)

3.4 | Retinal capillary densities and cerebral amyloid

To investigate the independence of *APOE* ε4 vascular effects from its known association with cerebral amyloidopathy, a gold-standard biomarker of AD pathology, we analyzed differences in retinal capillary densities in subjects with positive and negative amyloid PET scans in addition to analyses of continuous measures of cerebral amyloid (SUVR) with retinal capillary densities. We did not find significant differences in retinal capillary measures between amyloid positive (n = 16) and negative groups (n = 27; U = 186, P = .45 for VAD; U = 0.183, P = .41 for VSD). Adjusting for potential demographic confounders (age and sex) using a Kruskal-Wallis test did not change the findings ($\chi 2[1]$ = 0.57 P = .45 for VAD; $\chi 2[1]$ = 0.68 P = .41 for VSD; Figure 7A). Out of the total of 43 subjects, 32 had known *APOE* genotype (Table S1). Furthermore, regression of retinal VAD and VSD measures with a continuous measure of cerebral amyloid burden (18F-florbetapir SUVR, n = 33), controlling for age and sex, demonstrated no significant associations (VAD [r = 0.13, P = .49] and VSD [r = 0.12,P = .42]; Figure 7B).

4 | DISCUSSION

APOE ε4 genotype is the strongest common genetic risk factor for sporadic AD.[59] Understanding mechanisms by which *APOE* ε4 contributes to AD could provide novel therapeutic avenues and help with the understanding of AD pathogenesis.[60–62] In model systems, *APOE* ε4

has been shown to affect microvascular density and function.[14,15] The goal of this study was to test whether the noted effects of *APOE* ε4 on microvasculature in model systems translate to humans, and whether the effects can be detected, early, in cognitively asymptomatic individuals, upstream of clinically overt symptomatic neurodegenerative disease. Because brain microvasculature cannot be directly investigated in vivo in humans, retinal capillary density was used as a surrogate for brain capillaries. After controlling for systemic vascular risk factors and demographics, *APOE* ε4 carriers had lower retinal capillary density compared to non-carriers. Moreover, in light of interest in the characterization of early, asymptomatic disease stages, subjects with mild cognitive impairment or known neurodegenerative disease were excluded from primary analyses.

Genes interact with an individual's environment throughout the lifespan to give rise to phenotypes. Therefore, to assess whether *APOE* ε4 capillary effects are post-developmental and age dependent, linear regressions with age were conducted, demonstrating significant associations with retinal capillary density in *APOE* ε4 carriers. Because we used the retina as surrogate for the brain, we investigated the association of retinal capillary density with ASL, a non-invasive vascular brain imaging method that might reflect effects of capillary-level pathology. In this analysis we demonstrated that across all disease categories, from at risk asymptomatic individuals to those with dementia, retinal capillary density was significantly and specifically associated with brain perfusion—with higher retinal capillary density being associated with higher brain perfusion. Consistent with these findings, in mouse models of *APOE* ε4, brain capillary densities were found to be associated with ASL signal.[15] This suggests that retinal capillaries may be a valuable surrogate for brain capillaries. Of note, when all other risk factors are matched, the capillary differences could be observed on a single subject level. This is a strength of OCTA-derived capillary maps that are increasingly used for clinical monitoring of retinal vascular disease.

The goal of our study was not to test the spectrum of ophthalmological effects of *APOE*, which can be complex, but rather test its association with capillary changes in an organ directly related to the brain and accessible to direct imaging. To this end, we found that the effect sizes of group differences in retinal capillary density measures were substantial, such that up to 14% of the variance in retinal capillary density can be attributed to *APOE* genotype, independent of vascular risk factors. Work by Koronyo et al. suggests that it may be possible for amyloid to accumulate in the retina in the setting of cerebral amyloidopathy in AD.[63] However, the prevalence of retinal amyloidopathy and disease stage at which this may occur remain to be determined. In our current study, we have low suspicion that amyloidopathy is driving the differences noted in capillary densities and the associations of retinal capillary densities with CBF. To address this, we compared retinal capillary densities in a group of individuals with positive versus negative amyloid PET scans and found no differences in retinal capillary densities between the two groups. Nor did we find continuous associations of amyloid PET signal with retinal capillary densities. This suggests that capillary changes can occur early and independent of AD neuropathological biomarkers in *APOE* ε4 carriers. However, it should be noted that we did not have power to test possible interactions between amyloid and *APOE* ε4 on retinal capillaries, as amyloid imaging was only available for a subset of the sample. Additionally, in the case of amyloid, recent studies suggest pathogenic effects from oligomeric amyloid, rather than deposited plaques,[64] and PET-based analyses reported here are reflecting the presence of amyloid fibrils rather than amyloid oligomers. Additional limitations of our study included a cross-sectional study design and lack of AD biomarkers on all participants. Ultimately, longitudinal studies including all stages of clinical symptomatology and multi-modal biomarkers would shed further light on the relation of retinal vasculature in *APOE* ε4 gene carriers and non-carriers. In addition, inclusion of additional homozygote gene carriers to test potential dose effects, as well as other genetic risk factors for AD and other neurodegenerative disorders, would further help elucidate the biological bases of observed differences.

Overall, these findings provide the first report of lower retinal capillary densities in cognitively normal *APOE* ε4 carriers, and the relevance of these findings to brain microvasculature with associations of retinal capillary densities with a measure of CBF. This study provides insights into ways in which retinal vascular changes can be used as a surrogate measure for the study of vascular contributions to neurodegenerative disorders, starting from an at-risk stage. It is believed that therapeutic success in AD and other neurodegenerative disorders will require early interventions, with focus shifting from stages of overt clinical disease to at-risk asymptomatic or preclinical disease marked by the earliest detectable abnormalities in biomarkers.[65] This shift in perspective led to the drafting of biomarker-driven AD research diagnostic criteria that is based on A/T/(N) biomarkers (amyloid, tau, neurodegeneration).[66] However, mechanistic understanding of the many ways in which vascular disease can contribute to AD-associated neurodegeneration, cognitive impairment, and development of proteinopathies remains an important and active area of reseach.[67–72] To this end, better in vivo measures of vascular disease for incorporation into modeling disease progression and clinical symptomatology are urgently needed. If the success of interventions depends on early detection of disease, the in vivo markers of underlying pathology should capture all pathological processes associated with disease, and components such as vascular disease, including microangiopathy,[73–75] should be included. The capillary densities captured on OCTA could potentially contribute to microangiopathy measures in the studies of AD and related neurodegenerative disorders. Ultimately, impactful treatments for neurodegenerative disorders may require combinatorial therapies, addressing the multitude of age-associated pathologies that contribute to disease states and eventually functional decline and impairment. Our results indicate that retinal capillary measures merit further investigations as biomarkers of cerebral small vessel disease.

ACKNOWLEDGMENTS

We would like to thank patients and their families whose help and participation made this work possible. We also thank the National Centralized Repository for Alzheimer Disease and Related Dementias (NCRAD), for sample storage, which receives government support under a cooperative agreement grant (U24 AG21886) awarded by the National Institute on Aging (NIA). We thank Dr. William Jagust for

conducting PiB scans. Additionally, we thank contributors who collected samples used in this study, in addition to Drs. Eliana Marisa Ramos and Giovanni Coppola and Ms. Anna Karydas for assistance in obtaining genotypes, as well as the funding sources mentioned below for grants that have supported our work.

This study was supported by the following grants: Larry L. Hillblom start-up (2019A012SUP) and American Academy of Neurology fellowship to F.M.E.; UH2NS100614, UH3NS100614, R01EY030564, and unrestricted funding from Research to Prevent Blindness to the USC Department of Ophthalmology to A.H.K.; That Man May See and Hellman family funding to A.J.G., UH2NS100608, UH3NS100608, and Larry L. Hillblom Network Grant (2014-A-004-NET) to J.H.K.; NIH-NIA ADRC (P50 AG023501) and PPG (P01AG019724) to B.L.M., R01 (AG045611) to G.D.R., R01(s) (AG032289, AG048234), an Alzheimer's Association fellowship (AARF-16-443577) to R.L.J., and Larry L. Hillblom fellowship grant (2018-A-025-FEL) and NIH-NIA (K23AG061253) to A.M.S.

CONFLICTS OF INTEREST

The authors have no conflicts of interest to disclose with respect to the content presented in this manuscript. A.H.K. and F.M.E. note that they have received equipment from Carl Zeiss Meditec Inc in support of this study. In addition, A.H.K. has received grants, honoraria, and financial support from Carl Zeiss Meditec. G.D.R. receives research support from Avid Radiopharmaceuticals, Eli Lilly, GE Healthcare, and Life Molecular Imaging. G.D.R. has also received honoraria as a consultant for Axon Neurosciences, Eisai, and Merck, and speaking honoraria from GE Healthcare.

REFERENCES

1. Felsky D, Roostaei T, Nho K, et al. Neuropathological correlates and genetic architecture of microglial activation in elderly human brain. *Nat Commun*. 2019;10:1-12.
2. Busse M, Michler E, Von Hoff F, et al. Alterations in the peripheral immune system in dementia. *J Alzheimers Dis*. 2017;58:1303-1313.
3. Desikan RS, Schork AJ, Wang Y, et al. Polygenic overlap between C-Reactive protein, plasma lipids, and Alzheimer disease. *Circulation*. 2015;131:2061-2069.
4. Broce IJ, Tan CH, Fan CC, et al. Dissecting the genetic relationship between cardiovascular risk factors and Alzheimer's disease. *Acta Neuropathol*. 2019;137(2):209-226.
5. Belloy E, Napolioni V, Greicius MD. Review a quarter century of APOE and Alzheimer ' s disease : progress to date and the path forward. *Neuron*. 2019;101(5):820-838.
6. Patel D, Mez J, Vardarajan BN, et al. Association of rare coding mutations with Alzheimer disease and other dementias among adults of European ancestry. *JAMA Netw open*. 2019;2:e191350.
7. Schilling S, Tzourio C, Soumaré A, et al. Differential associations of plasma lipids with incident dementia and dementia subtypes in the 3C Study: a longitudinal, population-based prospective cohort study. *PLoS Med*. 2017;14:1-17.
8. Feeney C, Scott GP, Cole JH, Sastre M, Goldstone AP, Leech R. Seeds of neuroendocrine doubt. *Nature*. 2016;535:E1-E2.
9. G B. ApoE and cerebrovasculature in alzheimer's disease. *Neurodegener Dis*. 2015. https://doi.org/10.1159/000381736.
10. Farmer B, Kluemper J, Johnson L. Apolipoprotein E4 alters astrocyte fatty acid metabolism and lipid droplet formation. *Cells*. 2019;8:182.
11. Schneider JA, Bennett DA. Where vascular meets neurodegenerative disease. *Stroke*. 2010;41:1-6.
12. Liang WS, Reiman EM, Valla J, et al. Alzheimer's disease is associated with reduced expression of energy metabolism genes in posterior cingulate neurons. *Proc Natl Acad Sci USA*. 2008;105:4441-4446.
13. Schneider JA, Arvanitakis Z, Bang W, Bennett DA. Mixed brain pathologies account for most dementia cases in community-dwelling older persons. *Neurology*. 2007;69:2197-2204.
14. Bell RD, Winkler EA, Singh I, et al. Apolipoprotein e controls cerebrovascular integrity via cyclophilin A. *Nature*. 2012;485(7399):512-516.
15. Koizumi K, Hattori Y, Ahn SJ, et al. Apoε4 disrupts neurovascular regulation and undermines white matter integrity and cognitive function. *Nat Commun*. 2018;9(1):3816.
16. Gottesman RF, Albert MS, Alonso A, et al. Associations between midlife vascular risk factors and 25-year incident dementia in the Atherosclerosis Risk in Communities (ARIC) cohort. *JAMA Neurol*. 2017;74(10):1246-1254.
17. Arvanitakis Z, Capuano AW, Leurgans SE, Bennett DA, Schneider JA. Relation of cerebral vessel disease to Alzheimer's disease dementia and cognitive function in elderly people: a cross-sectional study. *Lancet Neurol*. 2016;15(9):934-943.
18. Ma Q, Zhao Z, Sagare AP, et al. Blood-brain barrier-associated pericytes internalize and clear aggregated amyloid-β42 by LRP1-dependent apolipoprotein e isoform-specific mechanism. *Mol Neurodegener*. 2018;13:1-13.
19. Fullerton SM, Shirman GA, Strittmatter WJ, Matthew WD. Impairment of the blood-nerve and blood-brain barriers in apolipoprotein E knockout mice. *Exp Neurol*. 2001;169(1):13-22.
20. Schmukler E, Michaelson DM, Pinkas-Kramarski R. The interplay between apolipoprotein E4 and the autophagic–endocytic–lysosomal axis. *Mol Neurobiol*. 2018;55(8):6863-6880.
21. Nortley R, Korte N, Izquierdo P, et al. Amyloid β oligomers constrict human capillaries in Alzheimer's disease via signaling to pericytes. *Science*. 2019;365(6450):eaav9518.
22. Salloway S, Gur T, Berzin T, et al. Effect of APOE genotype on microvascular basement membrane in Alzheimer's disease. *J Neurol Sci*. 2002;203-204:183-187.
23. Boyle PA, Yu L, Wilson RS, Leurgans SE, Schneider JA, Bennett DA. Person-specific contribution of neuropathologies to cognitive loss in old age. *Ann Neurol*. 2018;83(1):74-83.
24. Attems J, Jellinger KA. The overlap between vascular disease and Alzheimer's disease - lessons from pathology. *BMC Med*. 2014;12:1-12.
25. Kalaria RN, Ballard C. Overlap between pathology of Alzheimer disease and vascular dementia. *Alzheimer Dis Assoc Disord*. 1999;13 Suppl 3:S115-23.
26. Sweeney MD, Montagne A, Sagare AP, et al. Vascular dysfunction—The disregarded partner of Alzheimer's disease. *Alzheimer's Dement*. 2019;15:158-167.
27. Kashani AH, Chen CL, Gahm JK, et al. Optical coherence tomography angiography: a comprehensive review of current methods and clinical applications. *Prog Retinal Eye Res*. 2017;60:66-100.
28. Zhang A, Zhang Q, Chen C-L, Wang RK. Methods and algorithms for optical coherence tomography-based angiography: a review and comparison. *J Biomed Opt*. 2015;20(10):100901.
29. Wang RK, An L, Saunders S, Wilson DJ. Optical microangiography provides depth-resolved images of directional ocular blood perfusion in posterior eye segment. *J Biomed Opt*. 2010;15(2):020502.
30. Wang RK. Optical microangiography: a label-free 3-D imaging technology to visualize and quantify blood circulations within tissue beds in vivo. *IEEE J Sel Top Quantum Electron*. 2010;16(3):545-554.
31. Wang RK, Jacques SL, Ma Z, Hurst S, Hanson SR, Gruber A. Three dimensional optical angiography. *Opt Express*. 2007;15(7):4083-4097.

32. Ashimatey BS, Green KM, Chu Z, Wang RK, Kashani AH. Impaired retinal vascular reactivity in diabetic retinopathy as assessed by optical coherence tomography angiography. *Invest Ophthalmol Visual Sci*. 2019;60(7):2468-2473.
33. Bosch AJ, Harazny JM, Kistner I, Friedrich S, Wojtkiewicz J, Schmieder RE. Retinal capillary rarefaction in patients with untreated mild-moderate hypertension. *BMC Cardiovasc Disord*. 2017;17(1):300.
34. Querques G, Borrelli E, Sacconi R, et al. Functional and morphological changes of the retinal vessels in Alzheimer's disease and mild cognitive impairment. *Sci Rep*. 2019;9(1):63.
35. Chu Z, Lin J, Gao C, et al. Quantitative assessment of the retinal microvasculature using optical coherence tomography angiography. *J Biomed Opt*. 2016;21(6):66008.
36. Kim AY, Chu Z, Shahidzadeh A, Wang RK, Puliafito CA, Kashani AH. Quantifying microvascular density and morphology in diabetic retinopathy using spectral-domain optical coherence tomography angiography. *Invest Ophthalmol Visual Sci*. 2016;57(9):OCT362-70.
37. Kim AY, Rodger DC, Shahidzadeh A, et al. Quantifying retinal microvascular changes in uveitis using spectral-domain optical coherence tomography angiography. *Am J Ophthalmol*. 2016;171:101-112.
38. Koulisis N, Kim AY, Chu Z, et al. Quantitative microvascular analysis of retinal venous occlusions by spectral domain optical coherence tomography angiography. *PLoS One*. 2017;12(4):e0176404.
39. Staffaroni AM, Ljubenkov PA, Kornak J, et al. Longitudinal multimodal imaging and clinical endpoints for frontotemporal dementia clinical trials. *Brain*. 2019;142(2):443-459.
40. Alsop DC, Detre JA, Golay X, et al. Recommended implementation of arterial spin-labeled perfusion mri for clinical applications: a consensus of the ISMRM Perfusion Study group and the European consortium for ASL in dementia. *Magn Reson Med*. 2015;73(1):102-116.
41. Ashburner J, Friston KJ. Unified segmentation. *Neuroimage*. 2005;26(3):839-851.
42. Ashburner J, Friston KJ. Diffeomorphic registration using geodesic shooting and Gauss-Newton optimisation. *Neuroimage*. 2011;55(3):954-967.
43. Mazziotta JC, Toga AW, Evans A, Fox P, Lancaster J. A probabilistic atlas of the human brain: theory and rationale for its development. The International Consortium for Brain Mapping (ICBM). *Neuroimage*. 1995;2:89-101.
44. Desikan RS, Ségonne F, Fischl B, et al. An automated labeling system for subdividing the human cerebral cortex on MRI scans into gyral based regions of interest. *Neuroimage*. 2006;31:968-980.
45. Malone IB, Leung KK, Clegg S. Accurate automatic estimation of total intracranial volume: a nuisance variable with less nuisance. *Neuroimage*. 2015;104:366-372.
46. Du AT, Jahng GH, Hayasaka S, et al. Hypoperfusion in frontotemporal dementia and Alzheimer disease by arterial spin labeling MRI. *Neurology*. 2006;67:1215-1220.
47. Johnson NA, Jahng GH, Weiner MW, et al. Pattern of cerebral hypoperfusion in Alzheimer disease and mild cognitive impairment measured with arterial spin-labeling MR imaging: initial experience. *Radiology*. 2005;234:851-859.
48. Hayasaka S, Du AT, Duarte A, et al. A non-parametric approach for co-analysis of multi-modal brain imaging data: application to Alzheimer's disease. *Neuroimage*. 2006;30:768-779.
49. Jenkinson M, Beckmann CF, Behrens TEJ, Woolrich MW, Smith SM. FSL. *Neuroimage*. 2012;62:782-790.
50. Aguirre GK, Detre JA, Zarahn E, Alsop DC. Experimental design and the relative sensitivity of BOLD and perfusion fMRI. *Neuroimage*. 2002;15:488-500.
51. Avants BB, Epstein CL, Grossman M, Gee JC. Symmetric diffeomorphic image registration with cross-correlation: evaluating automated labeling of elderly and neurodegenerative brain. *Med Image Anal*. 2008;12:26-41.
52. Buxton RB, Frank LR, Wong EC, Siewert B, Warach S, Edelman RR. A general kinetic model for quantitative perfusion imaging with arterial spin labeling. *Magn Reson Med*. 1998;40:383-396.
53. Wang J, Aguirre GK, Kimberg DY, Roc AC, Li L, Detre JA. Arterial spin labeling perfusion fMRI with very low task frequency. *Magn Reson Med*. 2003;49:796-802.
54. Müller-Gärtner HW, Links JM, Prince JL, et al. Measurement of radiotracer concentration in brain gray matter using positron emission tomography: mRI-based correction for partial volume effects. *J Cereb Blood Flow Metab*. 1992;12:571-583.
55. Villeneuve S, Rabinovici GD, Cohn-Sheehy BI, et al. Existing Pittsburgh Compound-B positron emission tomography thresholds are too high: statistical and pathological evaluation. *Brain*. 2015;138(Pt 7):2020-2033.
56. Landau SM, et al. Amyloid-β imaging with Pittsburgh compound B and florbetapir: comparing radiotracers and quantification methods and initiative for the Alzheimer's disease neuroimaging. *Soc Nucl Med*. 2013. https://doi.org/10.2967/jnumed.112.109009.
57. Landau SM, Lu M, Joshi AD, et al. Comparing positron emission tomography imaging and cerebrospinal fluid measurements of β-amyloid. *Ann Neurol*. 2013;74(6):826-836.
58. Clark CM, Schneider JA, Bedell BJ, et al. Use of florbetapir-PET for imaging beta-amyloid pathology. *JAMA, J Am Med Assoc*. 2011;305:275-283.
59. Karch CM, Goate AM. Alzheimer's disease risk genes and mechanisms of disease pathogenesis. *Biol Psychiatry*. 2015;77:43-51.
60. Suidan GL, Ramaswamy G. Targeting apolipoprotein E for Alzheimer's disease: an industry perspective. *Int J Mol Sci*. 2019;20:2161.
61. Safieh M, Korczyn AD, Michaelson DM. ApoE4: an emerging therapeutic target for Alzheimer's disease. *BMC Med*. 2019;17:1-17.
62. Lin YT, Seo J, Gao F, et al. APOE4 causes widespread molecular and cellular alterations associated with Alzheimer's disease phenotypes in human iPSC-derived brain cell types. *Neuron*. 2018;98:1141-1154.
63. Koronyo Y, Biggs D, Barron E, et al. Retinal amyloid pathology and proof-of-concept imaging trial in Alzheimer's disease. *JCI insight*. 2017;2(16):e93621.
64. Beckman D, Ott S, Donis-Cox K, et al. Oligomeric Aβ in the monkey brain affects synaptic integrity and induces accelerated cortical aging. *Proc Natl Acad Sci USA*. 2019;116:26239-26246.in press.
65. Dubois B, Hampel H, Feldman HH, et al. Preclinical Alzheimer's disease: definition, natural history, and diagnostic criteria. *Alzheimers Dement*. 2016;12(3):292-323.
66. Jack CR, Bennett DA, Blennow K, et al. NIA-AA Research Framework: toward a biological definition of Alzheimer's disease. *Alzheimers Dement*. 2018;14:535-562.
67. Iturria-Medina Y, Sotero RC, Toussaint PJ, Mateos-Pérez JM, Evans AC. Alzheimer's Disease Neuroimaging Initiative. Early role of vascular dysregulation on late-onset Alzheimer's disease based on multifactorial data-driven analysis. *Nat Commun*. 2016;7:11934.
68. Merlini M, Rafalski VA, Coronado PER, et al. Fibrinogen induces microglia-mediated spine elimination and cognitive impairment in an Alzheimer ' s disease model report fibrinogen induces microglia-mediated spine elimination and cognitive impairment in an Alzheimer ' s disease model. *Neuron*. 2019;101:1099-1108.e6.
69. Ryu JK, Rafalski VA, Meyer-Franke A, et al. Fibrin-targeting immunotherapy protects against neuroinflammation and neurodegeneration. *Nat Immunol*. 2018;19:1212-1223.
70. Milikovsky DZ, Ofer J. Paroxysmal slow cortical activity in Alzheimer's disease and epilepsy is associated with blood-brain barrier dysfunction. *Sci Transl Med*. 2019;11(521):eaaw8954.
71. Senatorov VV Jr, Friedman AR, Milikovsky DZ, et al. Blood-brain barrier dysfunction in aging induces hyperactivation of TGFβ signaling and chronic yet reversible neural dysfunction. *Sci Transl Med*. 2019;11(521):eaaw8283.

72. Montagne A, Nation DA, Sagare AP, et al. APOE4 leads to blood–brain barrier dysfunction predicting cognitive decline. *Nature*. 2020;581(7806):71-76.
73. Snyder HM, Corriveau RA, Craft S, et al. Vascular contributions to cognitive impairment and dementia including Alzheimer's disease. *Alzheimers Dement*. 2015;11:710-717.
74. Bosetti F, Galis ZS, Bynoe MS, et al. Small blood vessels: big health problems?": scientific recommendations of the National Institutes of Health Workshop. *J Am Heart Assoc*. 2016;5:1-12.
75. Wardlaw JM, Smith C, Dichgans M. Small vessel disease: mechanisms and clinical implications. *Lancet Neurol*. 2019;4422:1-13.

SUPPORTING INFORMATION

Additional supporting information may be found online in the Supporting Information section at the end of the article.

How to cite this article: Elahi FM,, Ashimatey SB, Bennett DJ, et al. Retinal imaging demonstrates reduced capillary density in clinically unimpaired *APOE* ε4 gene carriers. *Alzheimer's Dement*. 2021;13:e12181.
https://doi.org/10.1002/dad2.12181